

Organic solar cell design as a function of radiative quantum efficiency

Blaise Godefroid and Gregory Kozyreff*

Optique Nonlinéaire Théorique, Université libre de Bruxelles (U.L.B.), CP 231, Belgium

(Dated: October 4, 2018)

We study the radiative decay, or fluorescence, of excitons in organic solar cells as a function of its geometrical parameters. Contrary to their non-radiative counterpart, fluorescence losses strongly depend on the environment. By properly tuning the thicknesses of the buffer layers between the active regions of the cell and the electrodes, the exciton lifetime and, hence, the exciton diffusion length can be increased. The importance of this phenomenon depends on the radiative quantum efficiency, which is the fraction of the exciton decay that is intrinsically due to fluorescence. Besides this effect, interferences within the cell control the efficiency of sunlight injection into the active layers. An optimal cell design must rely on the consideration of these two aspects. By properly managing fluorescence losses, one can significantly improve the cell performance. To demonstrate this fact, we use realistic material parameters inspired from literature data and obtain an increase of power conversion efficiency from 11.3% to 12.7%. Conversely, not to take into account the strong dependence of fluorescence on the environment may lead to a sub-optimal cell design and a degradation of cell performance. The presence of radiative losses, however small, significantly changes the optimal thicknesses. We illustrate this latter situation with experimental material data.

I. INTRODUCTION

Organic solar cells attract considerable research interest as a low-cost, mechanically flexible, and low-temperature manufactured alternative to inorganic solar cells. Various architectures exist, including donor/acceptor bilayer hetero-junction [1], bulk hetero-junction [2], tandem structure [3], and cascaded exciton-dissociating hetero-junctions [4]. One of the main factors that limits the efficiency of organic solar cells is the short diffusion length of excitons compared to the absorption length [5–7]. Indeed, because of the poor transport of photo-generated electrical excitations, the active layers are restricted to thicknesses that are too thin to fully absorb the incident sunlight. In order to overcome this difficulty, several photonic strategies have been devised to efficiently trap light: randomly structured interface [8], hexagonal arrays of nanocolumns [9, 10], nanoholes [11] or nanospheres [12, 13]. More recently, a photonic fiber plate was shown to significantly improve light trapping through intermittent ray chaos [14, 15]. While bulk hetero-junctions are an answer to the exciton transport problem, they come with additional difficulties, such as dead-ends in the path of electrons and holes towards their respective electrodes and chemical stability. Moreover, non-radiative recombinations at interfaces between the donor and acceptor are found to severely limit the efficiency of bulk hetero-junctions cells [16, 17]. Hence, bulk hetero-junctions are not a definitive solution to exciton transport and to increase the diffusion length of excitons in planar solar cells remains a critical objective.

Aside from material engineering, it has been pointed out that radiative losses (*i.e.* the diffusion length) can be optically engineered through the geometrical arrangement of the cell when this one is thin and hence present

microcavity effects [18]. Indeed, a radiating exciton is electromagnetically equivalent to an oscillating dipole. The optical power emitted by such a dipole can be increased or decreased in the proximity of boundaries, as was experimentally demonstrated by Drexhage [19]. A theoretical treatment of this radiation problem was worked out as early as 1909 by Sommerfeld in his study of antennas [20, 21]. More complete accounts followed Drexhage pioneering experiments, both theoretically [22–25] and experimentally [26, 27]. In high-Q cavities, it is well-known that spontaneous emission of radiation can be strongly suppressed [28]. As for solar cells, their are by construction poor cavities, in order to let as much light in as possible. Nevertheless, it was found that spontaneous emission, *i.e.* radiative losses, can still be significantly reduced. A general rule to promote this effect is to sandwich the photo-active layer by low-index regions. In particular, with n_1 and n_2 , the refractive indexes of the active layer and its surrounding, respectively, the rate of spontaneous emission can be reduced up to a factor $(n_2/n_1)^5$ for excitons with perpendicular orientation [18]. In addition to the above aspect, it has been emphasised that a proper choice of layer thicknesses inside the solar cell can significantly influence the distribution of sunlight intensity within the cell and, hence, the absorption of solar photon by the photo-active material [29–37].

The influence of exciton radiative losses on the device performance depends on the radiative quantum efficiency q , defined as

$$q = \frac{\Gamma_{r,\text{bulk}}}{\Gamma_{\text{bulk}}}, \quad \Gamma_{\text{bulk}} = \Gamma_{r,\text{bulk}} + \Gamma_{\text{nr}}, \quad (1)$$

where $\Gamma_{r,\text{bulk}}$ and Γ_{nr} are the rate of radiative and non-radiative decay, respectively, and the ‘bulk’ subscript indicate that it is the bulk value. The factor q is also called ‘fluorescence quantum efficiency’ or ‘photoluminescence quantum efficiency’. The bulk value of the radiative losses is an intrinsic quantity, which is obtained in

* blaise.godefroid@ulb.ac.be, gkozyreff@ulb.ac.be

the absence of boundary effects. In a confined environment such as in an organic cell, the actual radiative losses $\Gamma_r(z)$ generally differ from $\Gamma_{r,\text{bulk}}$ and depend on the position, z , of the exciton. The total losses can be written as

$$\Gamma(z, q) = \Gamma_{\text{bulk}} \left(1 - q + q \frac{\Gamma_r(z)}{\Gamma_{r,\text{bulk}}} \right). \quad (2)$$

In this paper, we seek to optimise the solar cell geometry taking both issues into account: efficient interference for sunlight absorption together with low exciton radiative losses. The fact that it is possible to reduce exciton emission while still efficiently admit light into the solar cell relies on two observations: The exciton emits light (i) at a well-defined frequency, and (ii) in all directions. Conversely, sunlight comes in a broad spectrum and enters the cell through a narrow cone around the normal direction. In Ref. [18], only the short-circuit current was evaluated, and a simplified incident spectrum was assumed, which did not allow one to evaluate the cell power conversion efficiency under a realistic illumination.

In order to assess device performance, we will first establish a generalisation of the Shockley-Queisser (S-Q) theory [38] for organic solar cells. Indeed, in this classic theory, the transport of electrical excitations is not an issue, since only inorganic semi-conductor materials with high charge mobilities are considered. Besides, microcavity effects are absent from S-Q theory. We will therefore generalise S-Q theory to take into account the diffusive exciton transport and microcavity effects both for sunlight injection and exciton radiation. In this more general theory, the External Quantum Efficiency (EQE), defined as the number of electrons generated per incoming photons, essentially replaces the material absorptivity.

The rest of the paper is organised as follows. In Sec. II, we present the generalised S-Q theory, taking into account exciton transport with space-dependent radiative losses. In Sec. III, we apply our theory to several cell geometries and discuss the impact of q on the optimal cell design. Finally, we conclude.

II. GENERALIZED SHOCKLEY-QUEISSER THEORY

A. Shockly-Queisser detailed balance theory for conventional solar cells

In its simplest form, S-Q theory of solar cells derives from the following statement of detailed balance:

$$I_s = I_R(V) + I(V). \quad (3)$$

Above, I_s is the number of electron-hole (e-h) pairs generated per unit of time and area by photon absorption. From this current, a portion $I_R(V)$ will recombine to produce a thermal electromagnetic radiation, leaving a particle current $I(V)$ (hence an electrical current $-eI(V)$)

of electrons to flow in the external circuit under an electrical potential V . For the sake of the present discussion, non-radiative recombination processes are omitted from the right hand side of Eq. (3).

If each absorbed photon leads to the generation of one and only one electron-hole pair then,

$$I_s = \Omega_s \int_0^\infty a(\lambda) \phi_{AM1.5}(\lambda) d\lambda \quad (4)$$

where $\Omega_s = 6.85 \times 10^{-5}$ is the solid angle under which illumination is received from the sun, $a(\lambda)$ is the absorptivity, $\phi_{AM1.5}$ is the AM1.5 solar spectrum (in photons $\text{s}^{-1}\text{m}^{-2}\text{m}^{-1}\text{sr}^{-1}$), and λ is the optical wavelength. We restrict our attention to illumination at normal incidence. Similarly, the recombination term is given by

$$I_R(V) = 2\pi \int_0^{\frac{\pi}{2}} \sin \theta \cos \theta \int_0^\infty a(\lambda) \phi(\lambda, T, V) d\lambda d\theta, \quad (5)$$

$$\phi(\lambda, T, V) = (2c/\lambda^4) \left[\exp\left(\frac{hc/\lambda - eV}{kT}\right) - 1 \right]^{-1}. \quad (6)$$

Above, $\phi(\lambda, T, V)$ is the Planck's distribution in which the chemical potential of radiation is given by eV [39–41], c is the speed of light, h is Planck's constant, k is Boltzmann's constant, and T is the cell temperature. In Eq. (5), we have used Kirchoff's law and equated the emissivity of the cell with its absorptivity. Thus, Eq. (3) becomes

$$I(V) = \int_0^\infty a(\lambda) [\Omega_s \phi_{AM1.5}(\lambda) - \pi \phi(\lambda, T, qV)] d\lambda. \quad (7)$$

This last equation eventually leads to the Shockley-Queisser's limit if we assume that $a(\lambda)$ is a step function. Stated in the above way, S-Q theory can simply be generalised to more general cell, such as those in which the internal electrical transport is controlled by excitons.

B. Exciton-regulated solar cell

In organic solar cells the absorption of a photon gives rise to an exciton, with a binding energy that is large compared to kT . The exciton are therefore long-lived; moreover, being electrically neutral, their motion is governed by diffusion. It is only at the interface between the donor and acceptor materials that the local electric gradient can break the exciton into a free hole and a free electron. Neglecting other processes, electron-hole pairs are only generated by exciton dissociation at the donor/acceptor interface and they subsequently disappear only by radiative recombination or by being collected in the external circuit. Thus, the detailed balance equation (3) becomes

$$I_X(\phi_{AM1.5}) = I(V) + I_R(V) \quad (8)$$

where $I_\chi(\phi_{AM1.5})$ is the exciton dissociation current under the AM1.5 illumination equal to the number of e-h pair generated per unit of time and area. This term is independent of voltage since excitons are neutral particles. It can be expressed as

$$I_\chi(\phi_{AM1.5}) = \Omega_s \int_0^\infty \text{EQE}(\lambda, 0) \phi_{AM1.5}(\lambda) d\lambda \quad (9)$$

where we define $\text{EQE}(\lambda, \theta)$ as the number of e-h pair generated per incident photon with wavelength λ and incidence angle θ with respect to the normal direction. This coincides with the usual definition if the charge collection efficiency is unity at short-circuit, which is a common assumption [29, 42].

Next, we must establish the radiative current $I_R(V)$. We first note that, in the dark, under an ambient isotropic illumination, $\phi(\lambda, T, 0)$, it must be equal to the e-h generation current, I_χ , as equilibrium conditions request.

$$I_R(0) = 2\pi \int_0^{\frac{\pi}{2}} \sin \theta \cos \theta \int_0^\infty \text{EQE}(\lambda, \theta) \phi(\lambda, T_c, 0) d\lambda d\theta \quad (10)$$

Outside equilibrium, the cell emits light with a potential of radiation as in Eq.(6). In that case, one postulates that Eq. (10) can be extrapolated to non-zero values of V as

$$I_R(V) = 2\pi \int_0^{\frac{\pi}{2}} \sin \theta \cos \theta \int_0^\infty \text{EQE}(\lambda, \theta) \phi(\lambda, T_c, V) d\lambda d\theta \quad (11)$$

The validity of this modelling step is discussed and confirmed in [43]. Note that this last expression is similar to Eq. (5) but with the absorptivity, $a(\lambda)$, replaced by $\text{EQE}(\lambda, \theta)$ [44]. Finally, Eq. (8) yields

$$I(V) = \Omega_s \int_0^\infty \text{EQE}(\lambda, 0) \phi_{AM1.5}(\lambda) d\lambda - 2\pi \int_0^{\frac{\pi}{2}} \sin \theta \cos \theta \int_0^\infty \text{EQE}(\lambda, \theta) \phi(\lambda, T_c, V) d\lambda d\theta \quad (12)$$

A similar derivation can be found in [45, 46]. Other phenomenological factors such as series and parallel resistances and the ideality factor are unnecessary for the present discussion and are therefore omitted from the model. Note that the theory so far is very general and is valid beyond the theory of organic cells. In order to determine the current-voltage curve (12) for a given cell, one has to calculate $\text{EQE}(\lambda, \theta)$. This is what we do in the next section for bilayer heterojunction organic solar cells.

C. Calculation of EQE

We now wish to compute $\text{EQE}(\lambda, \theta)$, *i.e.* the number of e-h pairs produced at the Donor/Acceptor interface per

incoming photon as a function of the photon wavelength and incidence angle.

Let $N(\lambda, \theta) = \phi_{AM1.5}(\lambda) \cos \theta$ be the number of photons that are incident per unit time and device area at an angle θ . This results in an electromagnetic intensity distribution $g(z, \lambda, \theta)$ inside the device, which can be computed by the transfer-matrix method [47, 48] (unpolarised light assumed.) With the proper normalisation for $g(z, \lambda, \theta)$ that takes into account the absorption coefficient and the conversion efficiency of absorbed photons into excitons, the rate of production of excitons per unit length is $N(\lambda, \theta)g(z, \lambda, \theta)$. Hence the distribution of excitons ρ produced by the flux $N(\lambda, \theta)$ satisfies

$$D \frac{\partial^2 \rho}{\partial z^2} - \Gamma(z, q) \rho + N(\lambda, \theta) g(z, \lambda, \theta) = 0, \quad (13)$$

with

$$\frac{\partial \rho}{\partial z} = 0, \quad z = z_{-1}, \quad (14a)$$

$$\rho = 0, \quad z = z_0, \quad (14b)$$

$$\frac{\partial \rho}{\partial z} = 0, \quad z = z_1. \quad (14c)$$

Above, D is the exciton diffusion constant, which takes the value D_A or D_D in the acceptor or donor material, respectively. Next, $\Gamma(z, q)$ is the exciton decay rate, which is computed as in [18] assuming random exciton orientation. Finally, Eqs. (14) express a no-flux boundary condition for excitons at the interfaces ($z = z_{\pm 1}$) between the active layers and the adjacent blocking layers, while $\rho(z_0) = 0$ models complete excitons dissociation into free electrons and holes at the Donor/Acceptor interface [29, 42, 49]. Exciton dissociation into free electrons and holes is assumed negligible anywhere else [50].

Note that if we divide Eq. (13) by Γ_{bulk} and normalise ρ as $\rho = (N/\Gamma_{\text{bulk}}) \rho'$, the exciton transport equation becomes

$$L^2 \frac{\partial^2 \rho'}{\partial z^2} - \frac{\Gamma(z, q)}{\Gamma_{\text{bulk}}} \rho' + g(z, \lambda, \theta) = 0, \quad L^2 = \frac{D}{\Gamma_{\text{bulk}}}. \quad (15)$$

Solving that equation, the diffusive current at the Donor/Acceptor interface yields the EQE as

$$\begin{aligned} \text{EQE}(\lambda, \theta) &= \frac{1}{N(\lambda)} \left(D_D \frac{\partial \rho}{\partial z} \Big|_{z_0+\epsilon} - D_A \frac{\partial \rho}{\partial z} \Big|_{z_0-\epsilon} \right) \\ &= L_D^2 \frac{\partial \rho'}{\partial z} \Big|_{z_0+\epsilon} - L_A^2 \frac{\partial \rho'}{\partial z} \Big|_{z_0-\epsilon}. \end{aligned} \quad (16)$$

Once, $\text{EQE}(\lambda, \theta)$ is determined, the $I(V)$ curve and the power conversion efficiency can be computed from Eq. (12).

III. NUMERICAL RESULTS

In this section, we illustrate our theory with two bi-layer cells, each one of the form

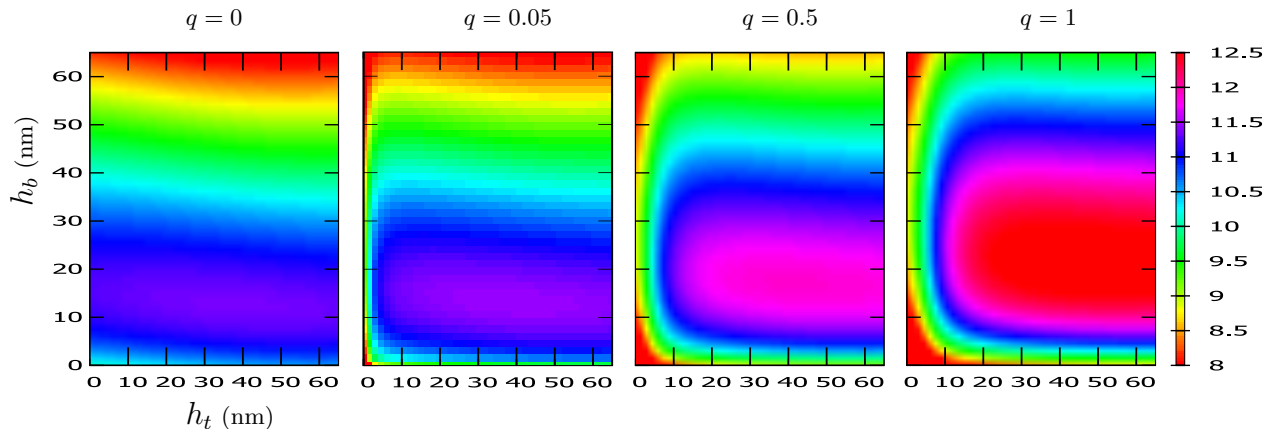


FIG. 1. (Color online) Power conversion efficiency η for the configuration presented in table I as a function of blocking layer thicknesses, h_t and h_b , for $q = 0, 0.05, 0.5, 1$ in both Acceptor and Donor layers.

Ag/HBL(h_b)/Acceptor/Donor/EBL(h_t)/ITO/glass.

Here, Ag designates the back silver electrode, HBL is a hole-blocking and electron-transporting layer, with thickness h_b , and EBL is an electron-blocking and hole-transporting layer, with thickness h_t . Finally, ITO designates a transparent indium tin oxide (ultra-thin metal film could be considered instead [37, 51] but we omit this possibility here, as this does not change the general conclusions.)

Given the large number of geometrical parameters available, we choose to maximise the cell power conversion efficiency by varying only the thickness h_b and h_t of the HBL and EBL, respectively, for given q . These two thicknesses are easily tunable fabrication parameters and it has been pointed out that they can significantly affect the efficiency of the cell [29–37].

As we vary q , we keep the bulk diffusion length unchanged, so as to compare active regions that would otherwise be equivalent. The power conversion efficiency is given by

$$\eta = \max_V [-eI(V)V] / \Omega_s \int_0^\infty (hc/\lambda) \phi_{AM1.5}(\lambda) d\lambda. \quad (17)$$

We consider two distinct situations. First, we demonstrate the potential benefit from using large- q photoactive organic molecules, if the cell is properly designed. To this end, we assume a favourable set of refractive indexes and thicknesses within ranges that are dictated by the literature. We show that a substantial gain in cell efficiency can be obtained.

Secondly, we simulate the following cell: Al/BCP/ C_{70} /DBP/ MoO_3 /ITO/glass, for which we use experimentally measured refractive indexes¹. Here, BCP stands for Bathocuproine and DBP for Tetraphenylidibenzoperiflanthene. The photovoltaic junction is achieved by C_{70} (Acceptor) and DBP (Donor). BCP and MoO_3 are electron and hole-transporting layer, respectively. In the study of this

latter cell, we simulate the possibility that C_{70} and DBP would be replaced by equivalent molecules, C_{70}^* and DBP^* , with identical complex refractive indexes and bulk diffusion lengths, but variable radiative quantum efficiency q . For this cell, the refractive indexes do not yield an increase of η with q . However, the optimal BCP and MoO_3 thicknesses do vary substantially with q .

In our computation of $\Gamma(z, q)$, we assumed that radiative excitons emit at 900nm. Further the distribution $g(z, \lambda, \theta)$ in Eq. (15) was computed by assuming that the incoming field was an even combination of TE and TM waves at oblique incidence. Finally, we assume the same value of q for the two active materials.

A. First example: high-efficiency cell

We first consider a favourable set of refractive indexes for increasing the diffusion length through the management of radiative losses. This set, together with layer thicknesses, is given in Table I. All refractive indexes are assumed independent of wavelength, except the imaginary part in the active layers, which is non-zero only between 300 and 700 nm. The assumed values of the refractive indexes for the blocking layers are consistent with the literature [29, 36, 52] and with the index of BCP. The

TABLE I. Optical parameters for an example cell. Imaginary part of refractive index in acceptor and donor layer non-zero only for $\lambda \in [300\text{nm}, 700\text{nm}]$

Layer	Thickness	Refractive index	Diffusion length
glass	∞	1.45	
ITO	150 nm	1.76+0.08i	
EBL	h_t	1.7	
Donor	15 nm	2.8+0.85i	10 nm
Acceptor	15 nm	2.8+0.85i	10 nm
HBL	h_b	1.7	
Ag	∞	0.03+ 5.19i	

¹ Courtesy of Jordi Martorell and Marina Mariano Juste

large index in the active region is chosen to maximise the contrast between the blocking and the photo-active layers, in accordance with the conclusion in Ref. [18]. A larger ratio of the real part of the refractive index in the photo-active layer and the blocking layers is liable to improve the cell efficiency. Furthermore, we assume an exciton diffusion length of 10 nm in both donor and acceptor layer, while the thickness of these layers is chosen to be 1.5 times the diffusion length. The ITO thickness of 150 nm is chosen so as to promote good light injection in the active layers thanks to constructive interferences in the spectral range of interest. To avoid spurious resonances in the glass capping, we assume this layer to have infinite thickness and correct the incoming intensity accordingly.

Figure 1 shows the cell efficiency as a function of the top and bottom blocking layer thicknesses, h_t and h_b for three values of q . One notices that there is a qualitative change in the graph as soon as $q > 0$, with low efficiency for very small values of either h_t or h_b . This is due to the quenching effect experienced by radiative excitons in the vicinity of a dissipative medium. As q progresses from $q = 0$ to $q = 1$, the optimal geometry vary from $(h_t, h_b) = (40 \text{ nm}, 12 \text{ nm})$ to $(h_t, h_b) = (45 \text{ nm}, 21 \text{ nm})$. Meanwhile the cell efficiency steadily progresses from 11.3% to 12.7%, see Fig. 2. For the most efficient configuration, we plot in Fig. 3, the space-dependent decay rate $\Gamma(z, q)$ for different values of q . In that figure, the advantage of managing the exciton radiative decay appears clearly.

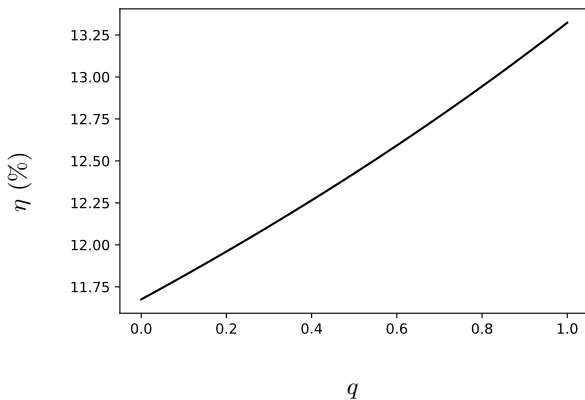


FIG. 2. Power conversion efficiency η as a function of radiative quantum efficiency q , for the parameters given in table I and $(h_t, h_b) = (45 \text{ nm}, 21 \text{ nm})$.

B. Second example: low efficiency cell

In this second example, we study the following cell, Al/BCP(h_b)/ C_{70}^* (31.5nm)/ DBP*(10.5nm)/ MoO_3 (h_t)/ITO(150nm)/ glass, where C_{70}^* and DBP* designate materials with identical complex refractive indexes to those

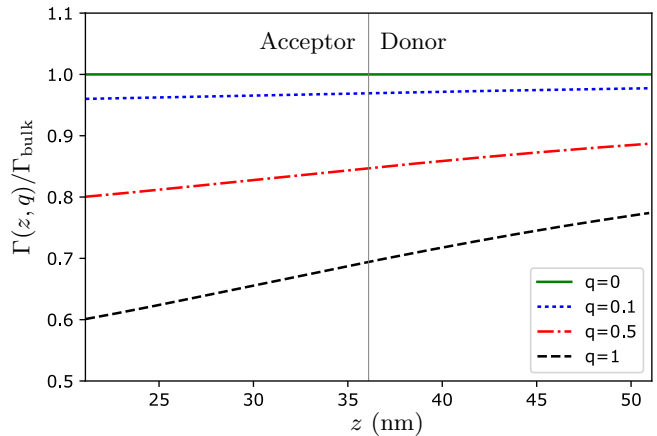


FIG. 3. (Color online) Normalised exciton decay rate as a function of the distance from the back electrode for the configuration presented in table I with $(h_t, h_b) = (45 \text{ nm}, 21 \text{ nm})$. The vertical line separates the Donor and Acceptor layers.

of C_{70} and DBP, but where q is a free parameter. According to Ref. [53], the diffusion length is 21nm in C_{70} and 7nm in DBP. As in the previous example, the C_{70}^* and DBP* thicknesses are chosen equal to 1.5 times the diffusion length, consistently with [54].

The graph of η as a function of h_b and h_t is given in Fig. 4 for four values of q . This time the maximum efficiency, 10.8%, is obtained for $q = 0$. The cell performance steadily degrades with increasing q , and do not exceed 10% for $q = 1$. However, it is important to note that the optimal configuration vary significantly between these extreme case: For $q = 0$, the best set is near of $(h_b, h_t) = (25 \text{ nm}, 0 \text{ nm})$; next, for $q = 0.05$ the optimal configuration is $(h_b, h_t) = (25 \text{ nm}, 9 \text{ nm})$; for $q = 0.5$ the optimal configuration is $(h_b, h_t) = (29 \text{ nm}, 15 \text{ nm})$; finally, for $q = 1$, it becomes $(h_b, h_t) = (32 \text{ nm}, 18 \text{ nm})$.

This last observation is a warning sign that the cell architecture should be designed with proper account of q . Indeed, with $(h_b, h_t) = (25 \text{ nm}, 0 \text{ nm})$, which is optimal for $q = 0$, η drops from 10.8% to 8.7% if $q = 0.5$ and is only 8.2% for $q = 1$, see Fig 5. The cause of this rapid decay can be understood from Fig. 6, which shows $\Gamma(z, q)$ for this configuration and various values of q . Here, boundary effects strongly increase the radiative losses in DBP*. While a reduction of radiative losses is achieved in C_{70}^* , this is not sufficient to counterbalance the adverse effect in DBP.

Looking again at Fig. 5, it is important to notice that there is a sudden drop of η as soon as q differs from zero, even if one keeps track of the best possible configuration (h_b, h_t) while varying q . This shows that to model the organic cell with $q = 0$ is an inaccurate modelling assumption.

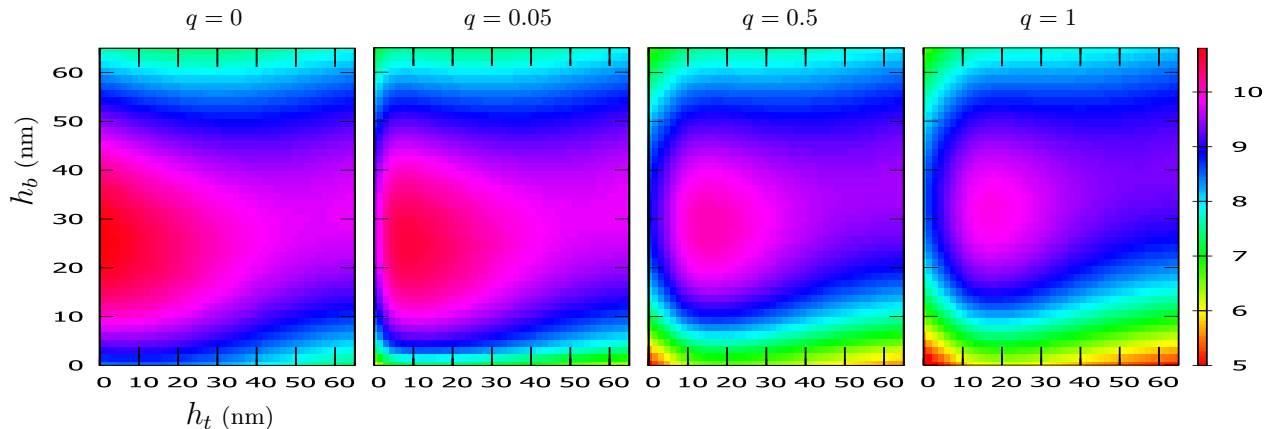


FIG. 4. (Color online) Power conversion efficiency η for Al/ BCP(h_b)/ C₇₀^{*}(31.5 nm)/ DBP^{*}(10.5 nm)/ MoO₃(h_t)/ ITO(150 nm)/ glass as a function of h_t and h_b for $q = 0, 0.05, 0.5, 1$ in both Acceptor and Donor layers.

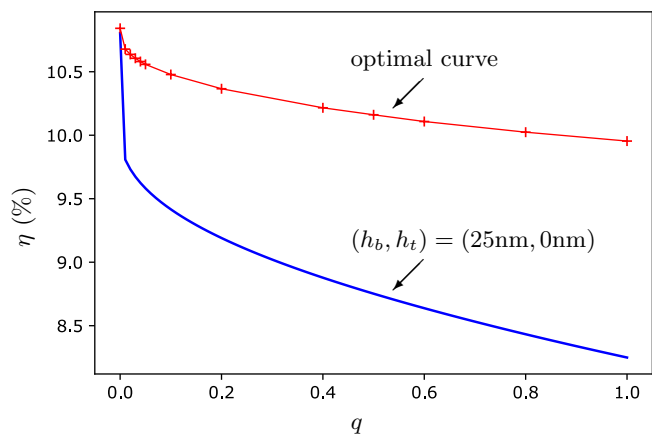


FIG. 5. (Color online) Power conversion efficiency η as a function of radiative quantum efficiency q , for Al/ BCP(h_b)/ C₇₀^{*}(31.5 nm)/ DBP^{*}(10.5 nm)/ MoO₃(h_t)/ ITO(150 nm)/ glass cell. Blue curve: $(h_b, h_t) = (25\text{nm}, 0\text{nm})$ for all q . Red curve: (h_b, h_t) set to optimal value for each q .

IV. DISCUSSION

In this paper, we have emphasised the importance of properly taking into account the space-dependent rate of radiative decay of exciton, $\Gamma(z, q)$ in organic solar cells. It is well-known that, as soon as the radiative quantum yield q is not zero, the radiative decay rate diverges as an exciton comes into contact with a dissipative surface [22], leading to exciton quenching. However, it has so far been overlooked that radiative decay can be reduced elsewhere in the cell. Here, we showed that with a proper choice of spacer thicknesses, h_b and h_t , this effects leads to a significant increase of the diffusion length and, hence, of the cell efficiency η . A general rule to exploit this effect is that the (real part of) refractive index contrast between the photoactive layers and the electron- and hole-blocking layers should be large. With a ratio of 2.8/1.7 and random exciton orientation, we have numerically demonstrated an increase of η from 11.3% in the

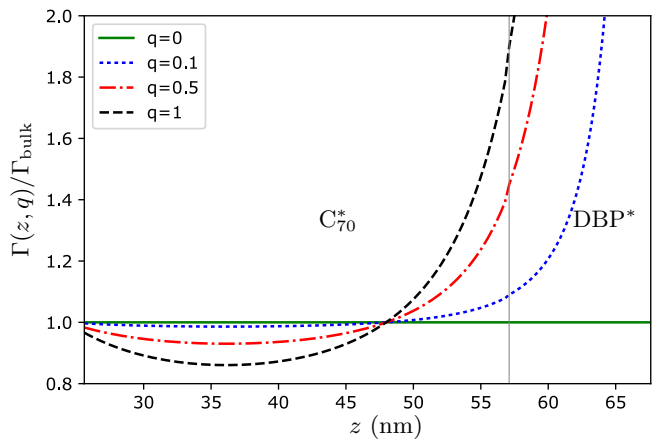


FIG. 6. (Color online) Normalised exciton decay rate in the active layers for different value of q for the following configuration: Al/ BCP(25 nm)/ C₇₀^{*}(31.5 nm)/ DBP^{*}(10.5 nm)/ MoO₃(0 nm)/ ITO(150 nm)/ glass. The vertical line separates the two active layers.

best configuration for $q = 0$ to 12.7% in the best configuration for $q = 1$. Note that the gain in efficiency rapidly increases with the refractive index in the active layers. If we suppose, for instance, that the blocking layers only has a refractive index of 1.45, then the maximum efficiency would increase from 11.3% with $q = 0$ to 14.3% with $q = 1$. Conversely, one may seek for active materials with larger refractive indexes. As an example, phthalocyanine (Pc) and its derivatives (subPc, Fluorinated-Pc, Mg-Pc, ...), or subnaphthalocyanine (subNc) can display refractive indexes above 3 and a large radiative quantum yield [55–60]. Equally, perovkites are found to display large refractive indexes in their absorption range [61] together with high photoluminescence efficiency [62]. Another way to drastically improve this gain would be to orient the exciton dipolar moment preferably along the cell axis, as this can dramatically decrease $\Gamma(z, q)$ [18].

Based on the above calculation, it would be desirable to develop organic solar cells with molecules having a large

q . In this regard, one may turn one's attention to organic light emitting devices (OLED) molecules. With OLEDs, substantial development have already been made to tailor the dipolar emission of excitons [63–65]. Moreover, q of nearly unity and good exciton orientation has been demonstrated [66]. However, contrary to maximising exciton emission, as in OLEDs, here we want to suppress it. The maximisation of η is found to require large spacers, both in order to maximise light injection and to suppress exciton decay. In practice, one is limited by the finite conductivity of these spacers. Nevertheless, large spacer values have been used in OLED [65] and also considered before in organic solar cells [31, 34, 36, 67, 68].

It has been claimed that a good solar cell must also be a good emitter [69]. Our conclusion above that solar cells can be improved based on good exciton radiative properties is consistent with this statement. However, it should be stressed that having a large value of q is not sufficient in itself to improve the cell efficiency. This is

what we demonstrated in our second numerical example. For refractive indexes corresponding to Al/ BCP/ C_{70} / DBP/ MoO_3 / ITO/ glass, a large value of q tends to degrade the cell performance, because radiative exciton decay is overall increased in the optimal configuration. Still, taking q into account appears crucial. Indeed, if not properly managed, radiative losses can be worse than anticipated. Thus, even in that case, q is an important parameter to take into account.

Acknowledgement

We thank Jordi Martorell and Marina Mariano Juste (ICFO, The Institute of Photonic Sciences) for helpful discussions and for communicating their data. G.K. is a research associate of the Fonds de la Recherche Scientifique -FNRS (Belgium)

-
- [1] C. W. Tang. Two-layer organic photovoltaic cell. *Appl. Phys. Lett.*, 48:183, 1986.
- [2] Sung Heum Park, Anshuman Roy, Serge Beaupré, Shinuk Cho, Nelson Coates, Ji Sun Moon, Daniel Moses, Mario Leclerc, Kwanghee Lee, and Alan J Heeger. Bulk heterojunction solar cells with internal quantum efficiency approaching 100%. *Nat. Photon.*, 3(5):297, 2009.
- [3] Tayebah Ameri, Gilles Dennler, Christoph Lungenschmied, and Christoph J Brabec. Organic tandem solar cells: a review. *Energ. Environ. Sci.*, 2(4):347–363, 2009.
- [4] Kjell Cnops, Barry P. Rand, David Cheyns, Bregt Verreert, Max A. Empl, and Paul Heremans. 8.4% efficient fullerene-free organic solar cells exploiting long-range exciton energy transfer. *Nat. Commun.*, 5:3406, 2014.
- [5] S. R. Forrest. The limits to organic photovoltaic cell efficiency. *MRS Bull.*, 30:28, 2005.
- [6] Bernard Kippelen and Jean-Luc Bredas. Organic photovoltaics. *Energ. Environ. Sci.*, 2:251, 2009.
- [7] Oleksandr V. Mikhnenko, Paul W. M. Blom, and Thuc-Quyen Nguyen. Exciton diffusion in organic semiconductors. *Energ. Environ. Sci.*, 8:1867–1888, 2015.
- [8] Eli Yablonovitch. Statistical ray optics. *J. Opt. Soc. Am. B*, 72(7):899–907, 1982.
- [9] Doo-Hyun Ko, John R Tumbleston, Lei Zhang, Stuart Williams, Joseph M DeSimone, Rene Lopez, and Edward T Samulski. Photonic crystal geometry for organic solar cells. *Nano Lett.*, 9(7):2742–2746, 2009.
- [10] Yingchi Liu, Christoph Kirsch, Abay Gadisa, Mukti Aryal, Sorin Mitran, Edward T Samulski, and Rene Lopez. Effects of nano-patterned versus simple flat active layers in upright organic photovoltaic devices. *J. Phys. D Appl. Phys.*, 46(2):024008, 2013.
- [11] Yu-Sheng Hsiao, Fan-Ching Chien, Jen-Hsien Huang, Chih-Ping Chen, Chiung-Wen Kuo, Chih-Wei Chu, and Peilin Chen. Facile transfer method for fabricating light-harvesting systems for polymer solar cells. *J. Phys. Chem. C*, 115(23):11864–11870, 2011.
- [12] Jonathan Grandier, Dennis M. Callahan, Jeremy N. Munday, and Harry A. Atwater. Light absorption enhancement in thin-film solar cells using whispering gallery modes in dielectric nanospheres. *Adv. Mater.*, 23:1272, 2011.
- [13] Yan Yao, Jie Yao, Vijay Kris Narasimhan, Zhichao Ruan, Chong Xie, Shanhui Fan, and Yi Cui. Broadband light management using low-q whispering gallery modes in spherical nanoshells. *Nat. Commun.*, 3:664, 2012.
- [14] Marina Mariano, Francisco J Rodríguez, Pablo Romero-Gomez, Gregory Kozyreff, and Jordi Martorell. Light coupling into the whispering gallery modes of a fiber array thin film solar cell for fixed partial sun tracking. *Sci. Rep.*, 4:4959, 2014.
- [15] Marina Mariano, Gregory Kozyreff, Luis G Gerling, Pablo Romero-Gomez, Joaquim Puigdollers, Jorge Bravo-Abad, and Jordi Martorell. Intermittent chaos for ergodic light trapping in a photonic fiber plate. *Light: Sci. Appl.*, 5(12):e16216, 2016.
- [16] Thomas Kirchartz, Kurt Taretto, and Uwe Rau. Efficiency limits of organic bulk heterojunction solar cells. *J. Phys. Chem. C*, 113:17958, 2009.
- [17] Dirk Veldman, Özlem Ipek, Stefan C. J. Meskers, Jörgen Sweelssen, Marc M. Koetse, Sjoerd C. Veenstra, Jan M. Kroon, Svetlana S. van Bavel, Joachim Loos, and René A. J. Janssen. Compositional and electric field dependence of the dissociation of charge transfer excitons in alternating polyfluorene copolymer/fullerene blends. *J. Am. Chem. Soc.*, 130(24):7721, 2008. PMID: 18494472.
- [18] G. Kozyreff, D. C. Urbanek, L.T. Vuong, O. Nieto Silleras, and J. Martorell. Microcavity effects on the generation, fluorescence, and diffusion of excitons in organic solar cells. *Opt. Express*, 21:A336–A354, 2013.
- [19] K. H. Drexhage. Interaction of light with monomolecular dye layers. In E. Wolf, editor, *Progress in Optics*, volume 12, pages 163 – 232. Elsevier, 1974.
- [20] A. Sommerfeld. Über die ausbreitung der wellen in der drahtlosen telegraphie. *Ann. der Physik*, 28:665–736,

- 1909.
- [21] A. Sommerfeld. *Partial Differential Equations in Physics*. Academic Press, 1949.
- [22] R. R. Chance, A. Prock, and R. Silbey. Molecular fluorescence and energy transfer near interfaces. *Adv. Chem. Phys.*, 37:1–65, 1978.
- [23] W. Lukosz. Theory of optical-environment-dependent spontaneous-emission rates for emitters in thin layers. *Phys. Rev. B*, 22(6):3030–3038, Sep 1980.
- [24] K. A. Neyts. Simulation of light emission from thin-film microcavities. *J. Opt. Soc. Am. A*, 15:962–971, 1998.
- [25] J.A.E. Wasey, A. Safonov, I.D.W. Samuel, and W.L. Barnes. Effects of dipole orientation and birefringence on the optical emission from thin films. *Opt. Commun.*, 183:109 – 121, 2000.
- [26] T. Tsutsui, C. Adachi, S. Saito, M. Watanabe, and M. Koishi. Effect of confined radiation field on spontaneous-emission lifetime in vacuum-deposited fluorescent dye films. *Chem. Phys. Lett.*, 182:143 – 146, 1991.
- [27] R. M. Amos and W. L. Barnes. Modification of the spontaneous emission rate of Eu^{3+} ions close to a thin metal mirror. *Phys. Rev. B*, 55:7249–7254, Mar 1997.
- [28] Daniel Kleppner. Inhibited spontaneous emission. *Phys. Rev. Lett.*, 47(4):233–236, Jul 1981.
- [29] Peter Peumans, Aharon Yakimov, and Stephen R. Forrest. Small molecular weight organic thin-film photodetectors and solar cells. *J. Appl. Phys.*, 93(7):3693–3723, 2003.
- [30] Seunghyup Yoo, William J. Potscavage Jr., Benoit Domercq, Sung-Ho Han, Tai-De Li, Simon C. Jones, Robert Szoszkiewicz, Dean Levi, Elisa Riedo, Seth R. Marder, and Bernard Kippelen. Analysis of improved photovoltaic properties of pentacene/ C_{60} organic solar cells: Effects of exciton blocking layer thickness and thermal annealing. *Solid State Electron.*, 51(10):1367 – 1375, 2007.
- [31] Jane Lee, Sei-Yong Kim, Changsoon Kim, and Jang-Joo Kim. Enhancement of the short circuit current in organic photovoltaic devices with microcavity structures. *Appl. Phys. Lett.*, 97(8):187, 2010.
- [32] Yongbing Long. Improving optical performance of low bandgap polymer solar cells by the two-mode moderate microcavity. *Appl. Phys. Lett.*, 98(3):12, 2011.
- [33] Yongbing Long. Red and near-infrared absorption enhancement for low bandgap polymer solar cells by combining the optical microcavity and optical spacers. *Sol. Energy Mater. Sol. Cells*, 95(12):3400–3407, 2011.
- [34] Rafael Betancur, Alberto Martínez-Otero, Xavier Elias, Pablo Romero-Gómez, Silvia Colodrero, Hernán Miguez, and Jordi Martorell. Optical interference for the matching of the external and internal quantum efficiencies in organic photovoltaic cells. *Sol. Energy Mater. Sol. Cells*, 104:87 – 91, 2012.
- [35] José-Francisco Salinas, Hin-Lap Yip, Chu-Chen Chueh, Chang-Zhi Li, José-Luis Maldonado, and Alex K-Y Jen. Optical design of transparent thin metal electrodes to enhance in-coupling and trapping of light in flexible polymer solar cells. *Adv. Mater.*, 24(47):6362, 2012.
- [36] Kung-Shih Chen, Hin-Lap Yip, José-Francisco Salinas, Yun-Xiang Xu, Chu-Chen Chueh, and Alex K-Y Jen. Strong photocurrent enhancements in highly efficient flexible organic solar cells by adopting a microcavity configuration. *Adv. Mater.*, 26(20):3349, 2014.
- [37] Chu-Chen Chueh, Michael Crump, and Alex K-Y Jen. Optical enhancement via electrode designs for high-performance polymer solar cells. *Adv. Funct. Mater.*, 26:321, 2015.
- [38] William Shockley and Hans J. Queisser. Detailed balance limit of efficiency of p-n junction solar cells. *J. Appl. Phys.*, 32:510–519, 1961.
- [39] P. Würfel. The chemical potential of radiation. *J. Phys. C: Solid State Phys.*, 15:3967–3985, 1982.
- [40] J. Nelson. *The Physics of Solar Cells*. Imperial College Press, 2003.
- [41] A. De Vos. *Thermodynamics of Solar Energy Conversion*. WILEY-VCH Verlag GmbH & Co. KGaA Weinheim, 2008.
- [42] Seunghyup Yoo, Benoit Domercq, and Bernard Kippelen. Efficient thin-film organic solar cells based on pentacene/ C_{60} heterojunctions. *Appl. Phys. Lett.*, 85:5427, 2004.
- [43] Thomas Kirchartz, Jenny Nelson, and Uwe Rau. Reciprocity between charge injection and extraction and its influence on the interpretation of electroluminescence spectra in organic solar cells. *Phys. Rev. Applied*, 5:054003, 2016.
- [44] Koen Vandewal, Zaifei Ma, Jonas Bergqvist, Zheng Tang, Ergang Wang, Patrik Henriksson, Kristofer Tvingstedt, Mats R. Andersson, Fengling Zhang, and Olle Inganäs. Quantification of quantum efficiency and energy losses in low bandgap polymer:fullerene solar cells with high open-circuit voltage. *Adv. Funct. Mater.*, 22:3480, 2012.
- [45] Uwe Rau. Reciprocity relation between photovoltaic quantum efficiency and electroluminescent emission of solar cells. *Phys. Rev. B*, 76:085303, 2007.
- [46] Uwe Rau, Beatrix Blank, Thomas CM Müller, and Thomas Kirchartz. Efficiency potential of photovoltaic materials and devices unveiled by detailed-balance analysis. *Phys. Rev. Applied*, 7:044016, 2017.
- [47] M. Born and E. Wolf. *Principle of Optics*. Pergamon, 1991.
- [48] Leif A. A. Pettersson, Lucimara S. Roman, and Olle Inganäs. Modeling photocurrent action spectra of photovoltaic devices based on organic thin films. *J. Appl. Phys.*, 86:487–496, 1999.
- [49] S. R. Scully and M. D. McGehee. Effects of optical interference and energy transfer on exciton diffusion length measurements in organic semiconductors. *J. Appl. Phys.*, 100:034907, 2006.
- [50] Thomas Stübinger and Wolfgang Brütting. Exciton diffusion and optical interference in organic donor–acceptor photovoltaic cells. *J. Appl. Phys.*, 90(7):3632–3641, 2001.
- [51] Jiang Huang, Chang-Zhi Li, Chu-Chen Chueh, Sheng-Qiang Liu, Jun-Sheng Yu, and Alex K.-Y. Jen. 10.4% power conversion efficiency of ITO-free organic photovoltaics through enhanced light trapping configuration. *Adv. Energy Mater.*, 5:1500406, 2015.
- [52] B. P. Rand, D. P. Burk, and S. R. Forrest. Offset energies at organic semiconductor heterojunction and their influence on the open-circuit voltage of thin-film solar cells. *Phys. Rev. B*, 75:115327, 2007.
- [53] Daisuke Yokoyama, Zhong Qiang Wang, Yong-Jin Pu, Kenta Kobayashi, Junji Kido, and Ziruo Hong. High-efficiency simple planar heterojunction organic thin-film photovoltaics with horizontally oriented amorphous donors. *Sol. Energy Mater. Sol. Cells*, 98:472 – 475, 2012.

- [54] Bernhard Siegmund, Muhammad T Sajjad, Johannes Widmer, Debdutta Ray, Christian Koerner, Moritz Riede, Karl Leo, Ifor DW Samuel, and Koen Vandewal. Exciton diffusion length and charge extraction yield in organic bilayer solar cells. *Adv. Mater.*, 29(12):1604424, 2017.
- [55] H. H. P. Gommans, D. Cheyns, T. Aernouts, C. Girotto, J. Poortmans, and P. Heremans. Electro-optical study of subphthalocyanine in a bilayer organic solar cell. *Adv. Funct. Mater.*, 17:2653–2658, 2007.
- [56] Michał Wojdyła, Waclaw Bała, Beata Derkowska, Mateusz Rebarz, and Andrzej Korcala. The temperature dependence of photoluminescence and absorption spectra of vacuum-sublimed magnesium phthalocyanine thin films. *Opt. Mat.*, 30(5):734–739, 2008.
- [57] Richard R. Lunt, Noel C. Giebink, Anna A. Belak, Jay B. Benziger, and Stephen R. Forrest. Exciton diffusion lengths of organic semiconductor thin films measured by spectrally resolved photoluminescence quenching. *J. Appl. Phys.*, 105:053711, 2009.
- [58] Bregt Verreet, Sarah Schols, David Cheyns, Barry P Rand, Hans Gommans, Tom Aernouts, Paul Heremans, and Jan Genoe. The characterization of chloroboron (iii) subnaphthalocyanine thin films and their application as a donor material for organic solar cells. *J. Mater. Chem.*, 19(30):5295–5297, 2009.
- [59] Bregt Verreet, Barry P. Rand, David Cheyns, Afshin Hadipour, Tom Aernouts, Paul Heremans, Anas Medina, Christian G. Claessens, and Tomas Torres. A 4% efficient organic solar cell using a fluorinated fused subphthalocyanine dimer as an electron acceptor. *Adv. Energy Mater.*, 1:565–568, 2011.
- [60] S Matthew Menke, Wade A Luhman, and Russell J Holmes. Tailored exciton diffusion in organic photovoltaic cells for enhanced power conversion efficiency. *Nat. Mater.*, 12(2):152, 2013.
- [61] Qianqian Lin, Ardalan Armin, Ravi Chandra Raju Nagiri, Paul L Burn, and Paul Meredith. Electro-optics of perovskite solar cells. *Nat. Photon.*, 9(2):106–112, 2015.
- [62] Felix Deschler, Michael Price, Sandeep Pathak, Lina E Klintberg, David-Dominik Jarausch, Ruben Higler, Sven Httner, Tomas Leijtens, Samuel D Stranks, Henry J Snaith, et al. High photoluminescence efficiency and optically pumped lasing in solution-processed mixed halide perovskite semiconductors. *J. Phys. Chem. Lett.*, 5(8):1421–1426, 2014.
- [63] Michael Flämmich, Malte C. Gather, Norbert Danz, Dirk Michaelis, and Klaus Meerholz. In situ measurement of the internal luminescence quantum efficiency in organic light-emitting diodes. *Appl. Phys. Lett.*, 95:263306, 2009.
- [64] Michael Flämmich, Malte C. Gather, Norbert Danz, Dirk Michaelis, Andreas H. Bräuer, Klaus Meerholz, and Andreas Tünnermann. Orientation of emissive dipoles in oleds: Quantitative in situ analysis. *Org. Electron.*, 11:1039 – 1046, 2010.
- [65] L. Penninck, F. Steinbacher, R. Krause, and K. Neyts. Determining emissive dipole orientation in organic light emitting devices by decay time measurement. *Org. Electron.*, 13:3079 – 3084, 2012.
- [66] Sei-Yong Kim, Won-Ik Jeong, Christian Mayr, Young-Seo Park, Kwon-Hyeon Kim, Jeong-Hwan Lee, Chang-Ki Moon, Wolfgang Brütting, and Jang-Joo Kim. Organic light-emitting diodes with 30% external quantum efficiency based on a horizontally oriented emitter. *Adv. Funct. Mater.*, 23(31):3896–3900, 2013.
- [67] Brian E Lassiter, Guodan Wei, Siyi Wang, Jeremy D Zimmerman, Viacheslav V Diev, Mark E Thompson, and Stephen R Forrest. Organic photovoltaics incorporating electron conducting exciton blocking layers. *Appl. Phys. Lett.*, 98(24):112, 2011.
- [68] MZ Sahdan, MF Malek, MS Alias, SA Kamaruddin, CA Norhidayah, N Sarip, N Nafarizal, and M Rusop. Metamorphosis of the zno buffer layer thicknesses on the performance of inverted organic solar cells. *J. Mater. Sci. Mater. Electron.*, 27(12):12891–12902, 2016.
- [69] Owen D Miller and Eli Yablonovitch. Photon extraction: the key physics for approaching solar cell efficiency limits. In *SPIE NanoScience+ Engineering*, page 880807. International Society for Optics and Photonics, 2013.